Radiology

Efficacy and Safety of MR Imaging with Liver-specific Contrast Agent: U.S. Multicenter Phase III Study[1]

David A. Bluemke, MD, PhD
Dushyant Sahani, MD
Marco Amendola, MD
Thomas Balzer, MD
Josy Breuer, MD
Jeffrey J. Brown, MD
David D. Casalino, MD
Peter L. Davis, MD
Isaac R. Francis, MD
Glenn Krinsky, MD
Fred T. Lee, Jr, MD
David Lu, MD
Erik K. Paulson, MD
Lawrence H. Schwartz, MD
Evan S. Siegelman, MD
for the Group

Published online before print
10.1148/radiol.2371031842
Radiology 2005; 237:89–98

Abbreviation:
EOB-DTPA = ethoxybenzyl diethylenetriamine pentaacetic acid

[1] From the Johns Hopkins University School of Medicine, 600 N Wolfe St, Baltimore, MD 21287 (D.A.B.). The complete list of authors and affiliations is at the end of this article. Received November 18, 2003; revision requested February 6, 2004; revision received November 18; accepted December 30. Supported by Berlex Laboratories. **Address correspondence to** D.A.B.

See Materials and Methods for pertinent disclosures.

Author contributions:
Guarantors of integrity of entire study, D.A.B., K.S., J.B.; study concepts, K.S., J.B., T.B.; study design, all authors; literature research, D.A.B., K.S., J.B.; clinical studies, D.A.B., M.A., J.J.B., D.D.C., P.L.D., I.R.F., G.K., F.T.L., D.L., E.K.P., D.S., L.H.S., E.S.S., W.C.S., T.M.W., A.W.; data acquisition and analysis/interpretation, all authors; statistical analysis, J.B.; manuscript preparation and definition of intellectual content, all authors; manuscript editing, D.A.B., J.B., K.S.; manuscript revision/review and final version approval, all authors

PURPOSE: To assess prospectively the efficacy and safety of postcontrast magnetic resonance (MR) imaging with gadolinium ethoxybenzyl diethylenetriamine pentaacetic acid (Gd-EOB-DTPA) compared with that of precontrast MR imaging in patients who are known to have or are suspected of having liver lesions and who are scheduled for hepatic surgery.

MATERIALS AND METHODS: Investigational review board approval and written informed consent were obtained. HIPAA went into effect after data collection. A total of 172 patients were enrolled. After precontrast MR imaging, 169 patients (94 men, 75 women; mean age, 61 years; age range, 19–84 years) received an intravenous bolus of 25 μmol/kg Gd-EOB-DTPA and underwent dynamic gradient-recalled-echo and delayed MR imaging 20 minutes after injection. Arterial and portal phase computed tomography (CT) were performed within 6 weeks of MR imaging. The standard of reference was surgery with intraoperative ultrasonography (US) and biopsy and/or pathologic evaluation of resected liver segments and/or 3-month follow-up of nonresected segments if intraoperative US was not available. Three blinded reviewers and unblinded site investigators identified liver lesions on segment maps. The Wilcoxon signed rank test was used to compare differences in per-patient sensitivity of precontrast and postcontrast MR images. Adverse events were recorded, and patient monitoring and laboratory assay were performed at time of injection and up to 24 hours after contrast material administration.

RESULTS: At MR imaging, 316 lesions were identified in 131 patients. In 77% (P = .012), 72% (P = .15), and 71% (P = .027) of patients for readers 1, 2, and 3, respectively, more lesions were seen at precontrast and postcontrast MR imaging combined than at precontrast MR imaging alone. Sensitivity values for blinded readings were significantly greater at postcontrast MR imaging than at precontrast MR imaging for two of three blinded readers. For all blinded readers, combined precontrast and postcontrast MR images showed no difference in sensitivity compared with helical CT scans. The use of MR imaging, however, yielded fewer patients with at least one false-positive lesion (37%, 31%, and 34% of patients for readers 1, 2, and 3, respectively) than did helical CT (45%, 36%, and 43% of patients for readers 1, 2, and 3, respectively).

CONCLUSION: Compared with precontrast MR imaging, postcontrast MR imaging with Gd-EOB-DTPA demonstrated improved sensitivity for lesion detection in the majority of blinded readers, with no substantial adverse events.
© RSNA, 2005

Gadolinium (Gd) ethoxybenzyl diethylenetriamine pentaacetic acid (Gd-EOB-DTPA) is a T1 contrast agent for magnetic resonance (MR) imaging that has several advantageous properties for evaluating the liver. After injection, rapid and specific hepatocyte uptake with biliary excretion occurs in approximately 50% of the injected dose. As a result of hepatocyte uptake, normal areas of liver exhibit T1 shortening, whereas focal liver lesions, such as hepatic metastases, do not exhibit T1 shortening. Mangafodipir trisodium, which

is another contrast agent that is approved for use in the United States, has similar T1 shortening and parenchymal enhancement properties (1,2) but is not administered as a bolus injection. A bolus injection of Gd-EOB-DTPA followed by arterial and portal phase imaging may prove to be more useful than the administration of other contrast agents, such as mangafodipir trisodium and ferumoxides, which allow only delayed phase imaging. In addition to arterial and portal phase imaging for the detection and characterization of liver lesions, hepatic arterial and portal vein status can be evaluated. Vascular assessment, together with parenchymal imaging, can provide a comprehensive evaluation of hepatic disease.

The safety and dosing of Gd-EOB-DTPA have previously been evaluated in phase I and II clinical studies (3,4). Doses of up to 100 μmol/kg Gd-EOB-DTPA have been well tolerated, with maximal parenchymal enhancement occurring 20 minutes after injection (4,5). Biliary excretion is rapid and can be detected within 10 minutes of injection. Doses of 25 and 50 μmol/kg Gd-EOB-DTPA have shown hepatic enhancement similar to that of 0.1 mmol/kg gadolinium diethylenetriaminepentaacetic acid (Gd-DTPA) during dynamic MR imaging (6). Delayed imaging with Gd-EOB-DTPA, however, was superior to Gd-DTPA for the detection and characterization of lesions (6).

The purpose of this phase III multicenter clinical study was to assess prospectively the efficacy and safety of postcontrast MR imaging with Gd-EOB-DTPA compared with that of precontrast MR imaging in patients who were known to have or were suspected of having liver lesions and who were scheduled to undergo hepatic surgery.

MATERIALS AND METHODS

Funding for this study was provided by Berlex Laboratories. Authors who were not employees of Berlex Laboratories controlled the inclusion of any data or information that might have presented a conflict of interest for those who were employees of Berlex Laboratories.

The primary efficacy variable for this study was the per-patient sensitivity of liver lesion detection at MR imaging before and after Gd-EOB-DTPA administration. The safety of Gd-EOB-DTPA was assessed by means of patient monitoring and blood serum assay at the time of and up to 24 hours after contrast material administration.

Patient Population

Patients 18 years of age or older who had liver lesions and were scheduled to undergo liver surgery were included in the study. Patients were excluded if they had contraindications to MR imaging (eg, aneurysm clip, pacemaker, or severe claustrophobia). Additional exclusion criteria were *(a)* women who were pregnant or lactating, *(b)* patients who had received any investigational drug within 30 days prior to entering this study, *(c)* patients who had received any radiographic contrast material 24 hours before or after Gd-EOB-DTPA injection, *(d)* patients who had received any liver-specific contrast agent within 2 weeks prior to Gd-EOB-DTPA injection, *(e)* patients who had received iodized oil at any time or who were scheduled to receive iodized oil, *(f)* patients who were clinically unstable, *(g)* patients who had a history of anaphylactic reaction to any allergen, drug, or contrast agent, and *(h)* patients who were scheduled to undergo liver biopsy 24 hours before or after Gd-EOB-DTPA injection. The 24-hour exclusion for biopsy after Gd-EOB-DTPA injection was used because safety monitoring continued for 24 hours after injection and because an intervening biopsy may otherwise have confounded the safety results. In addition, patients who underwent local or systemic liver tumor therapy within 2 weeks before imaging or who planned to undergo local therapy between the time of the required computed tomographic (CT) or MR imaging examination were excluded. Patients who were scheduled to undergo or had undergone upper abdominal surgery between CT and MR imaging or who had received Gd-EOB-DTPA in any prior investigational study were also excluded. The investigational review board at each institution approved the protocol, and all patients provided written informed consent. The Health Insurance Portability and Accountability Act went into effect after our data collection was completed. Patient anonymity, however, was maintained.

A total of 172 patients were enrolled between September 1998 and April 2000. Enrolling centers included New York University Medical Center, New York, NY (one patient); University of Miami School of Medicine, Miami, Fla (23 patients); Mallinckrodt Institute of Radiology, St Louis, Mo (11 patients); University of Chicago Hospital, Chicago, Ill (one patient); Presbyterian University Hospital, Pittsburgh, Pa (nine patients); Johns Hopkins Hospital, Baltimore, Md (30 patients); University of Michigan Hospitals, Ann Arbor, Mich (20 patients); Duke University Medical Center, Durham, NC (13 patients); University of California, Los Angeles Hospital, Los Angeles, Calif (20 patients); Emory University Hospital, Atlanta, Ga (six patients); Massachusetts General Hospital, Boston, Mass (26 patients); and University of Alabama, Birmingham, Ala (12 patients).

Gd-EOB-DTPA Administration

Patients received 25 μmol/kg (0.1 mL/kg) Gd-EOB-DTPA as an intravenous bolus injection, which was administered at a rate of 2 mL/sec. The bolus injection was followed by a saline flush that was sufficient to clear the intravenous line. If the dose was incomplete, the total volume of the injected dose was recorded. The imaging protocol that was performed following injection is discussed later.

Patient Monitoring

Physical examination of the patient was performed by the principal site investigator within 24 hours before and 24 hours after Gd-EOB-DTPA administration. Vital signs were assessed immediately before and 5 minutes after injection, immediately after completion of the MR examination, and 4 and 24 hours after Gd-EOB-DTPA injection.

Adverse Events

Adverse events were defined as illnesses and signs or symptoms that either appeared or worsened after the implementation of the study procedures, independent of any drug other than contrast material. Patient monitoring began 24 hours prior to Gd-EOB-DTPA administration and ended 24 hours after Gd-EOB-DTPA administration. Adverse events were classified as either nonserious or serious, and the intensity of the event was rated as mild, moderate, or severe. Serious events were those events that were life threatening, were permanently disabling, caused death, required hospitalization, or extended inpatient hospitalization.

Laboratory Testing

A complete blood count and serum assay were performed within 24 hours before, 2–4 hours after, and 20–28 hours after Gd-EOB-DTPA injection. In addition to a complete blood count, measure-

ments of serum glucose, creatinine, uric acid, urea nitrogen, calcium, phosphorus, total protein, albumin, total bilirubin alkaline phosphatase, sodium, potassium, chloride, and lactic dehydrogenase were obtained. Measurements of clotting function included prothrombin time and activated partial thromboplastin time. Hepatic function was assessed by measuring γ-glutamyl transpeptidase, aspartate aminotransferase, and alanine aminotransferase levels. Urinalysis consisted of leukocyte, erythrocyte, total protein, and albumin measurement. Clinical laboratory analyses were performed at a central laboratory.

MR Imaging

MR imaging was performed by using a phased-array surface coil for signal reception. Commercially available 1.5-T MR imagers and pulse sequences were used in the study. Precontrast transverse T2-weighted fast spin-echo images were obtained with ≥3000/90–120 (repetition time msec/echo time msec), two to four signals acquired, matrix size of 192–256 × 256, field of view of ≤400 mm, section thickness of 5–8 mm, intersection gap of 0–2 mm, and chemical shift fat suppression. Precontrast and postcontrast transverse dynamic spoiled gradient-recalled-echo T1-weighted images were obtained with 100–200/2.2–2.4, flip angle of 70°–80°, matrix size of 160–192 × 256, field of view of ≤400 mm, section thickness of 5–8 mm, intersection gap of 0–2 mm, and breath-hold acquisition. The acquisition of dynamic gradient-recalled-echo images was simultaneous with the start of contrast material injection and was repeated five times consecutively, with 30 seconds between each acquisition to allow breathing. At 20 minutes after contrast material injection, the T1-weighted gradient-recalled-echo sequence was repeated.

CT Scanning

Arterial and portal phase postcontrast helical CT, as well as MR imaging and hepatic surgery, were performed within the same 6-week period. CT was performed with a section thickness of 5–8 mm, pitch of 1–2, iodinated contrast material injection rate of 3–5 mL/sec, craniocaudal scanning, 100–150 kV, and 180–300 mAs. Arterial phase imaging began 25–35 seconds after contrast material injection, and portal phase imaging began 45–70 seconds after contrast material injection.

Image Analysis

The principal site investigators, who had 3–20 years experience in hepatic imaging (G.K., M.A., J.J.B., D.D.C., P.L.D., D.A.B., I.R.F., E.K.P., D.L., W.C.S., T.M.W.), conducted CT and MR image review at each center. Site investigators were not blinded to any imaging, pathologic, or laboratory result that was relevant to the patient's care. Investigators recorded the number, diameter, and diagnosis of each lesion. A maximum of up to 15 individual lesions were recorded per patient. If more than 15 lesions of the same type (eg, metastases) were present, the group of lesions was classified as "more than 15 lesions," without further specification of the number of lesions. If a patient had more than 15 regenerating nodules or cysts, but other lesions were also present, a maximum of up to 15 other lesions were recorded.

Three independent blinded readers (E.S.S., F.T.L., and L.H.S., with 11, 14, and 14 years experience in hepatic imaging, respectively) who had not participated in MR imaging conducted blinded image review. Blinded readers did not have information as to the patients' age, race, sex, name, or hospital and did not know the diagnosis of the lesion or which device the patients were imaged with. Blinded readers were also not told if the images were obtained before or after contrast material administration. Pulse sequence parameters (eg, repetition time, echo time, flip angle, and matrix size) were available to the readers. The readers were aware that the patients were known to have or were suspected of having liver lesions. Different reading sessions were conducted to evaluate *(a)* helical CT scans alone, *(b)* precontrast and postcontrast T1-weighted MR images alone, or *(c)* precontrast and postcontrast T1-weighted and T2-weighted MR images alone. Images were presented to the readers for interpretation on imaging workstations.

Site investigators and blinded reviewers identified lesions by using maps that contained eight sections of the liver, which were drawn according to the Couinaud system of liver anatomy (7). Lesion maps were recorded for MR imaging, helical CT, intraoperative ultrasonography (US), pathologic analysis, and/or 3-month diagnostic follow-up (explained further in Standard of Reference section). Blinded readers indicated the liver segment that contained the lesion, as well as the adjacent segment if the lesion crossed segment boundaries. In addition, the lesion diameter was recorded to aid in lesion identification.

Standard of Reference

The standard of reference for the final diagnosis was one or more of the following: surgery with intraoperative US and pathologic evaluation of the resected liver segments or intraoperative US alone if hepatic resection was not performed. If intraoperative US was not available for the nonresected liver segments, an additional diagnostic and/or therapeutic procedure, including CT, MR imaging, US, or biopsy, was performed within 3 months after MR imaging. The type of additional diagnostic and/or therapeutic procedure that was performed had to be different than that which was used to detect the lesion. The investigator at each site recorded the final diagnosis on the basis of these standards of reference.

Lesion Tracking

Lesion tracking, as opposed to considering only the total number of lesions present per patient, was performed to ensure that the detected lesion corresponded to the lesion that was identified with the standard of reference. A matched lesion was defined as a reader-identified lesion that had an identical location within the same liver segment, as seen on respective CT and MR images and verified with the standard of reference. Both an independent blinded radiologist who was not a site investigator and a blinded reader identified each lesion by using imaging procedures that were able to match the location of the lesions identified with the standard of reference based on the recorded liver maps.

Statistical Analysis

The primary efficacy variable of both unblinded and blinded readings was the per-patient sensitivity of lesion detection at diagnostic imaging (ie, helical CT and MR imaging) for matched lesions that were verified by means of the standard of reference. True-positive lesions were defined as lesions that were detected at CT or MR imaging and were verified with the standard of reference. For each patient, the sensitivity was calculated as the relative frequency with which lesions that were identified with the standard of reference were matched by using the two diagnostic imaging procedures. To compare the two diagnostic procedures, the difference between the corresponding

relative frequencies was calculated for each patient.

The null hypothesis of the primary statistical assessment was that the sensitivity of precontrast MR images was equal to that of the combined precontrast and postcontrast MR images. The comparison of precontrast MR images and combined MR images was based on differences between per-patient sensitivities (paired differences). The Wilcoxon signed rank test was applied at a two-sided significance level of 5%. The correlation of lesions within the same patient was accounted for by estimating sensitivity on a per-patient basis and by using these estimates for the evaluation with the Wilcoxon signed rank test. A secondary analysis was performed to compare *(a)* postcontrast MR imaging with helical CT, *(b)* precontrast MR imaging with postcontrast MR imaging, *(c)* precontrast and postcontrast MR imaging with helical CT, *(d)* precontrast and postcontrast MR imaging with postcontrast MR imaging, and *(e)* postcontrast T1-weighted MR imaging with precontrast T1-weighted MR imaging.

The κ values for multiple readers were used to evaluate the agreement between blinded readers for the overall lesion detection rate and for the classification of lesions as benign or malignant.

As a measure of specificity, the number of false-positive lesions was determined. False-positive lesions were defined as lesions that were detected during any of the imaging examinations but were not verified with the standard of reference.

For analysis of safety, the frequency of adverse events was recorded. For clinical laboratory evaluation, laboratory values that demonstrated clinically relevant changes from the baseline, as determined by the site investigator, were tabulated.

RESULTS

Patient Enrollment

Three patients did not receive Gd-EOB-DTPA, two patients withdrew consent owing to claustrophobia during the precontrast MR imaging, and one patient had precontrast MR images with severe metal artifacts. Therefore, 169 patients received Gd-EOB-DTPA and were included in the adverse event analysis. The mean age of all patients was 61 years (age range, 19–84 years). A total of 94 (55.6%) of 169 patients were men, and 75 (44.4%) were women. Of 169 patients who received Gd-EOB-DTPA, 142 (84.0%) were white, 12 (7.1%) were black, 12 (7.1%) were Hispanic, and three (1.8%) were Asian. Thirteen (7.7%) of 169 patients had a history of cirrhosis. Reasons for planned hepatic surgery are listed in Table 1 according to diagnosis.

Adverse Events

There were no serious adverse events nor did any adverse event lead to a discontinuation of the study. Overall, there were 28 adverse events reported in 17 (10.0%) of 169 patients after the injection of Gd-EOB-DTPA. One of these events (injection site reaction) was classified as definitely contrast material-related. Fourteen adverse events (three cases of vasodilatation, two cases of headache, two cases of dyspnea, and one case each of increased sweating, palpitation, taste alteration, dizziness, back pain, parosmia, and injection site edema) in nine patients were assessed as probably or possibly contrast material-related. The remainder of the adverse events were classified by the site investigators as unlikely or not contrast material-related. All adverse events (15 events in 10 patients) that were definitely, probably, or possibly contrast material-related were mild or moderate in intensity.

Clinical Laboratory Evaluation

Laboratory values that demonstrated clinically relevant changes from the baseline, as judged by the site investigator, were recorded in seven (4.1%) of 169 patients. One patient had abnormally low total protein and inorganic phosphate levels at 24-hour follow-up for reasons that were unknown to the site investigator. These tests were repeated 4 days later, and the values had returned to normal. This patient had a history of breast cancer, had undergone chemotherapy, and had received digoxin, quinapril, fluoxetine, and alprazolam as concomitant medications. Another patient had elevated albumin (27.9 g/mol creatinine) and decreased sodium (132 mmol/L) levels at 24-hour urinalysis. Both levels returned to baseline at follow-up 4 days later. This patient had a history of alcohol-induced liver cirrhosis and hepatocellular carcinoma and had received lactulose, metoprolol, methylphenidate (Ritalin; Novartis, East Hanover, NJ), and dyazide as concomitant medications. The other five patients had abnormal values that were determined by site investigators to be related to the patients' underlying medical history and/or concomitant medication.

TABLE 1
Reasons for Planned Hepatic Surgery according to Diagnosis

Diagnosis	No. of Patients (n = 169)
Metastasis	108 (63.9)
Hepatocellular carcinoma	33 (19.5)
Hemangioma	8 (4.7)
Cholangiocarcinoma	7 (4.1)
Adenoma	2 (1.2)
Liver cyst	1 (0.6)
Hydatic cyst	1 (0.6)
Other	9 (5.3)

Note.—Numbers in parentheses are percentages.

Overall Lesion Detection

Site investigators.—Of the 169 patients, 31 (18.3%) did not undergo a standard of reference procedure. Seven additional patients had major protocol deviations: Three patients did not undergo a valid follow-up procedure, two patients were missing 20 minutes of their postcontrast MR images, one patient underwent surgery more than 6 weeks after the MR imaging with Gd-EOB-DTPA, and one patient received less than 80% of the Gd-EOB-DTPA dose and was excluded from the MR image evaluation. Thus, imaging data from 131 patients were available for the efficacy analysis.

A total of 316 lesions were identified in 131 patients (mean, 2.4 lesions per patient; range 0–10 lesions). Ninety-eight (31.0%) of 316 lesions were <1 cm in diameter, and 218 (69.0%) of 316 lesions were ≥1 cm in diameter. In five patients, no lesions were identified with the standard of reference. Of the 126 patients with lesions, four patients did not undergo valid helical CT; therefore, 122 patients with 299 lesions that were identified with the standard of reference were included in the analysis of CT data.

Table 2 presents the number of matched lesions identified by the site investigators at precontrast MR imaging, postcontrast MR imaging, and helical CT. A total of 197 (65.9%) of 299 lesions were identified at helical CT, 198 (62.6%) of 316 were identified at precontrast MR imaging, and 224 (70.9%) of 316 were identified at postcontrast MR imaging. Similar trends were present for lesions ≥1 cm and for lesions <1 cm in diameter (Table 2).

Blinded readers.—Table 3 shows the overall lesion detection rate for each of the blinded readers. For all three readers, the number of matched lesions identified

TABLE 2
Number of Lesions Identified as Hepatocellular Carcinoma or Metastases by Unblinded Site Investigators at MR Imaging and Helical CT

Modality	All Lesions	Hepatocellular Carcinoma		Metastases	
		<1 cm	≥1 cm	<1 cm	≥1 cm
Precontrast MR imaging	198/316 (62.7)	0/7 (0)	22/26 (85)	16/49 (33)	113/140 (80.7)
Postcontrast MR imaging	224/316 (70.9)	0/7 (0)	22/26 (85)	22/49 (45)	123/140 (87.8)
Helical CT	197/299 (65.9)	1/7 (14)	22/23 (96)	12/40 (30)	112/136 (82.4)

Note.—Numbers in parentheses are percentages.

TABLE 3
Number of Liver Lesions Classified as Hepatocellular Carcinoma and Metastasis by Blinded Readers at MR Imaging and Helical CT

Modality	All Lesions*	Hepatocellular Carcinoma		Metastasis	
		<1 cm	≥1 cm	<1 cm	≥1 cm
		Reader 1			
Precontrast MR imaging					
T1-weighted and T2-weighted	200/316 (63.3)	0/33	23/33	16/189	107/189
T1-weighted	163/316 (51.6)	0/33	17/33	13/189	95/189
Postcontrast MR imaging					
T1-weighted and T2-weighted	234/316 (74.0)	0/33	23/33	28/189	116/189
T1-weighted	205/316 (64.9)	0/33	21/33	23/189	111/189
Pre- and postcontrast MR imaging	226/316 (71.5)	0/33	23/33	27/189	113/189
Helical CT	210/299 (70.2)	1/30	21/30	20/176	109/176
		Reader 2			
Precontrast MR imaging					
T1-weighted and T2-weighted	195/316 (61.7)	1/33	21/33	16/189	106/189
T1-weighted	170/316 (53.8)	0/33	16/33	15/189	96/189
Postcontrast MR imaging					
T1-weighted and T2-weighted	213/316 (67.4)	0/33	23/33	23/189	117/189
T1-weighted	189/316 (59.8)	0/33	21/33	22/189	109/189
Pre- and postcontrast MR imaging	215/316 (68.0)	0/33	20/33	23/189	112/189
Helical CT	201/299 (67.2)	1/30	19/30	16/176	114/176
		Reader 3			
Precontrast MR imaging					
T1-weighted and T2-weighted	187/316 (59.2)	0/33	21/33	14/189	99/189
T1-weighted	166/316 (52.5)	0/33	19/33	15/189	90/189
Postcontrast MR imaging					
T1-weighted and T2-weighted	209/316 (66.1)	0/33	25/33	18/189	111/189
T1-weighted	192/316 (60.8)	0/33	23/33	16/189	106/189
Pre- and postcontrast MR imaging	215/316 (68.0)	0/33	23/33	22/189	113/189
Helical CT	188/299 (62.9)	0/30	20/33	12/176	111/176

* Numbers in parentheses are percentages.

on combined precontrast and postcontrast MR images exceeded the number of lesions identified on precontrast MR images and helical CT scans by 6%–9% for precontrast MR images and 1%–5% for helical CT scans. For reader 1, the greatest number of lesions was identified on the postcontrast MR images. For readers 2 and 3, the greatest number of lesions was identified on the combined precontrast and postcontrast MR images.

Per-Patient Sensitivity Analysis

The primary efficacy analysis compared the per-patient sensitivity of lesion detection on precontrast and postcontrast MR images combined with the per-patient sensitivity of lesion detection on precontrast MR images alone. A total of 126 patients had lesions that were identified by using the standard of reference. Of these, 31, 29, and 41 patients for readers 1, 2, and 3, respectively, showed a difference between the number of matched lesions detected on precontrast and postcontrast MR images combined and those detected on precontrast MR images alone. In 24 (77%) of 31 (P = .012), 21 (72%) of 29 (P = .15), and 29 (71%) of 41 (P = .027) patients for readers 1, 2, and 3, respectively, more lesions were correctly seen on the precontrast and postcontrast MR images combined than were seen on precontrast MR images alone when compared with the standard of reference. Thus, statistically significant results in favor of the combined precontrast and postcontrast MR images were obtained for two of three blinded readers.

Secondary comparisons were conducted for both unblinded (site) and blinded readings to compare the per-patient lesion detection rate for MR images obtained with Gd-EOB-DTPA with that of other image combinations (Figs 1, 2).

Table 4 lists the comparisons that were performed and the sensitivity values. For unblinded readings, the sensitivity values of postcontrast MR images were significantly greater than those of precontrast MR images and helical CT scans. For blinded readings, sensitivity values of postcontrast MR images were significantly greater than those of precontrast MR images in two of three readers (Table 4). In addition, postcontrast T1-weighted MR imaging demonstrated a higher sensitivity than precontrast T1-weighted imaging in one of three readers.

Specificity Analysis

A total of 35 (26.7%) of 131 patients at precontrast MR imaging, 41 (31.3%) of 131 at postcontrast MR imaging, and 40 (31.5%) of 127 at helical CT had at least one false-positive lesion (benign or malignant) that was identified by unblinded site investigators. Table 5 shows the number of patients with at least one false-positive lesion for the blinded readers. For all three readers, the use of precontrast and postcontrast MR images combined yielded fewer patients with at least one false-positive lesion than did helical CT scans alone. At least one false-positive lesion was seen in an additional five (4%) of 131 and two (2%) of 131 patients for readers 1 and 2, respectively, for precontrast and postcontrast MR images combined versus precontrast MR images alone (Table 5). Reader 3 reported five (4%) of 131 fewer patients with at least one false-positive lesion of precontrast and postcontrast MR images combined versus precontrast MR images alone.

Table 6 shows the number of false-positive lesions for both unblinded site investigators and blinded readers. Postcontrast MR images demonstrated a higher number of false-positive lesions than did the precontrast MR images for all three blinded readers. Also, all three blinded readers reported a higher number of false-positive lesions for helical CT scans than for precontrast and postcontrast MR images combined. This was primarily because there was a higher number of false-positive lesions that measured <1 cm at helical CT.

The majority of false-positive lesions were classified by unblinded site readers as malignant (Table 6). The percentage of malignant lesions was similar for helical CT, precontrast MR imaging, and postcontrast MR imaging. Blinded readers 1 and 2 classified the majority of false-positive lesions as malignant for all imaging combinations except for helical CT (reader 2). Reader 3 classified fewer false-positive lesions as malignant (Table 6) but correspondingly classified more lesions as "not assessable" (data not shown).

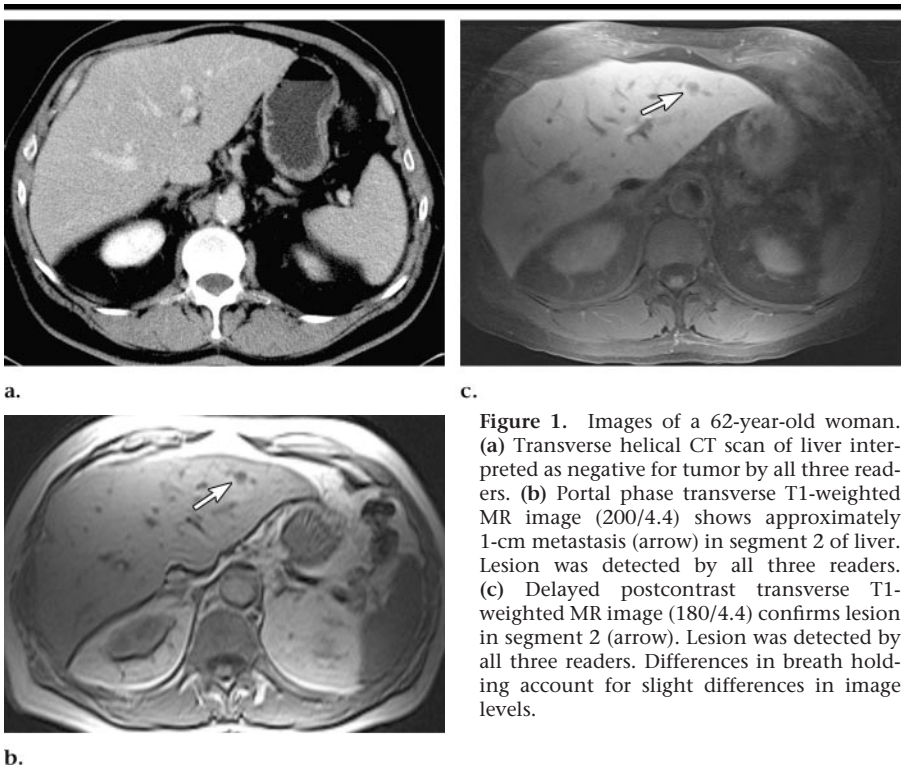

Figure 1. Images of a 62-year-old woman. **(a)** Transverse helical CT scan of liver interpreted as negative for tumor by all three readers. **(b)** Portal phase transverse T1-weighted MR image (200/4.4) shows approximately 1-cm metastasis (arrow) in segment 2 of liver. Lesion was detected by all three readers. **(c)** Delayed postcontrast transverse T1-weighted MR image (180/4.4) confirms lesion in segment 2 (arrow). Lesion was detected by all three readers. Differences in breath holding account for slight differences in image levels.

Lesion Classification

A total of 316 lesions were identified by using the standard of reference. Of these, 232 (73.4%) lesions were malignant, while 79 (25.0%) were benign. Five (1.6%) lesions were not assessable. Table 7 shows the number of lesions correctly detected and classified as benign or malignant by the blinded readers. Compared with precontrast MR images and helical CT scans, postcontrast MR images were used by the unblinded site readers to correctly classify more lesions as malignant (178 [76.7%] of 232 lesions) or benign (57 [72.2%] of 79 lesions). For all blinded readers, the use of postcontrast MR images alone and precontrast and postcontrast MR images combined resulted in a higher percentage of correctly classified lesions than did the use of helical CT scans or precontrast MR images alone (Table 7). For all blinded readers, the differences in the number of lesions that were correctly classified by using the combined precontrast and postcontrast MR images versus CT scans were larger for benign lesions than for malignant lesions (Table 7).

Reader Agreement

Reader agreement was assessed for the 316 lesions that were identified at MR imaging and were verified with the standard of reference and for the 297 lesions that were identified at helical CT and were verified with the standard of reference. The agreement between readers for lesion detection was highest at precontrast MR imaging ($\kappa = 0.69$) compared with postcontrast MR imaging, combined MR imaging, and helical CT ($\kappa = 0.64, 0.58, 0.54$, respectively). The agreement between readers for classification of a lesion as benign or malignant was highest at postcontrast MR imaging ($\kappa = 0.66$) compared with precontrast MR imaging, combined MR imaging, and helical CT ($\kappa = 0.65, 0.62, 0.57$, respectively).

DISCUSSION

In our study, for unblinded site investigators and all blinded readers, 6%–9% more lesions were detected with precontrast and postcontrast MR imaging combined than were detected with precontrast MR imaging alone. Lesion detection was improved for lesions ≥1 cm and for lesions <1 cm. This difference was statistically significant for site investigators and for two of three blinded reviewers. Improved lesion detection was associated

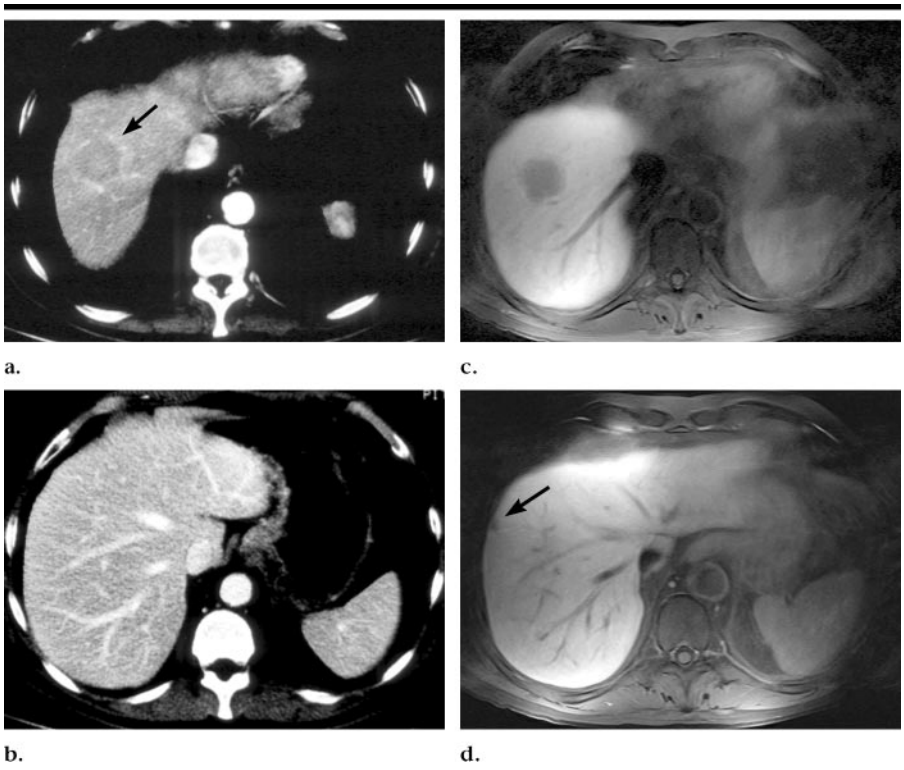

Figure 2. Images of a 57-year-old man. **(a)** Transverse helical CT scan near dome of liver shows approximately 3-cm lesion owing to metastasis (arrow). Lesion was not detected by two of three readers. **(b)** Transverse helical CT scan several centimeters below **a** was interpreted as negative for tumor by all three readers. **(c)** Delayed postcontrast transverse T1-weighted MR image (200/4.4) at same level as **a** shows hypointense lesion owing to metastasis. Lesion was detected by all readers. **(d)** Delayed postcontrast transverse T1-weighted MR image (180/4.4) at same level as **b** shows 1-cm lesion (arrow) that was confirmed as metastasis. Lesion was detected by two of three readers. Differences in breath holding account for slight differences in image levels.

with a small (2%–3%) increase in the number of patients with at least one false-positive lesion for two of the blinded readers and a similar decrease in false-positive lesions for one blinded reader.

Findings from helical CT were compared with those from postcontrast MR imaging, and no significant difference in lesion detection (sensitivity) between the two modalities was observed. For all blinded readers, however, the number of patients with one false-positive lesion was 5%–9% less with precontrast and postcontrast MR imaging combined than with helical CT alone. The percentage of lesions that were correctly classified as malignant or benign was 2%–15% greater for blinded readers who compared precontrast and postcontrast MR images with helical CT scans. False-positive lesions may potentially affect patient care by altering plans for surgery, particularly if the positive lesions are identified in separate liver lobes. The effect of false-positive lesions on patient care, however, has changed to some degree as a result of newer approaches to liver surgery. Traditional surgical exclusion criteria, such as more than four liver lesions, are no longer strict contraindications to surgery. Nonanatomic hepatic resections and combined therapy, including radiofrequency ablation, provide surgeons with several options for the surgical treatment of liver disease. Surgical procedures that begin as exploration of the liver but instead show lack of resectable liver disease may be used to allow placement of a hepatic artery infusion pump. Thus, surgical management of liver disease has become more flexible, in part because of imperfect noninvasive preoperative imaging and advances in surgical techniques.

Gd-EOB-DTPA has considerable potential advantages for MR imaging of the liver. The results of CT scanning with iodinated contrast agents and the results of MR imaging with gadolinium chelate have led to an understanding of the importance of capturing arterial and portal phase enhancement characteristics of liver lesions. A bolus injection of these contrast agents is also necessary to assess hepatic artery and portal vein status. Delayed imaging with Gd-EOB-DTPA results in the specific uptake of the contrast agent by hepatocytes. The contrast agent is then excreted into the biliary system, allowing assessment of biliary anatomy in combination with established MR cholangiographic techniques (8,9).

Gadolinium chelates that are currently approved for MR imaging of the liver by the Food and Drug Administration in the United States have a low rate of minor adverse events (10,11). The excellent safety profile of these contrast agents establishes a base of comparison and expectation for new MR contrast agents. The results of our study, which was similar to prior phase I and II clinical studies (3,4), demonstrate that Gd-EOB-DTPA was well tolerated, with no substantial adverse events. Minor adverse events (eg, headache and vasodilatation) that were potentially related to the administration of contrast material were reported in 10 (5.9%) of 169 patients. Importantly, none of the adverse events was rated as severe in intensity.

The stated sensitivities and specificities of postcontrast MR imaging for the detection of focal liver lesions vary widely in the literature. For example, the results of a multicenter trial comparing gadoversetamide with gadopentetate dimeglumine indicate sensitivities of 58.3% and 59.5%, respectively (12). Results of single center studies have demonstrated sensitivities greater than 90% (13–16). These variations are in part related to the study design but are also related to the varying methods of stating specificity for lesion detection. For this reason, CT scanning was included as a reference standard and was compared with MR imaging. In this study, all mapped lesions were carefully tracked by an independent radiologist in an attempt to match the findings from surgery, intraoperative US, MR imaging, and CT. Although the sensitivity of postcontrast MR imaging that we have reported is low (68%–71% for blinded readers), similar values have been described in other multicenter studies (1,2,17).

As expected, the sensitivities of blinded readings were lower than those of unblinded readings by 7%–10% for MR imaging and 3%–7% for CT. Unblinded investigators were aware of the lesion diagnosis and of any comparison examinations that were performed prior to MR imaging or CT. There may also be certain imaging characteristics of the MR imagers or CT scanners at each site that would allow the site readers to be more

TABLE 4
Per-Patient Sensitivity of Liver Lesion Detection for Unblinded Site Investigators and Blinded Readers at MR Imaging and Helical CT

Comparison	Unblinded Site Investigators		Reader 1		Reader 2		Reader 3	
	Sensitivity	*P* Value	Sensitivity	*P* Value	Sensitivity	*P* Value	Sensitivity	*P* Value
Postcontrast vs precontrast MR imaging	15/15 (100)	<.001	26/29 (90)	<.001	24/34 (70)	<.028	25/36 (69)	.07
Postcontrast MR imaging vs helical CT	16/22 (73)	<.01	22/31 (71)	<.06	17/34 (50)	<.29	29/47 (62)	.61
Pre- and postcontrast MR imaging vs helical CT	···	···	20/36 (56)	<.53	16/35 (46)	<.13	27/45 (60)	.59
Pre- and postcontrast MR imaging vs postcontrast MR imaging	···	···	10/28 (36)	<.12	10/25 (40)	<.40	11/23 (48)	.52
Postcontrast T1-weighted vs precontrast T1-weighted MR imaging	···	···	34/41 (83)	<.001	25/42 (60)	<.60	34/48 (71)	.10

Note.—Numbers in parentheses are percentages. Denominators represent the number of patients in whom there was a difference between the number of lesions detected with the two comparison modalities. The numerator represents the number of patients in whom the first examination demonstrated more lesions than did the second examination. If the percentage was less that 50%, then the second examination yielded a higher number of detected lesions in more patients. For MR imaging comparisons, results of 126 patient examinations were available. For MR imaging vs CT comparisons, results of 122 patient examinations were available for both modalities.

TABLE 5
Number of Patients with at Least One False-Positive Lesion for Blinded Readings at MR Imaging and Helical CT

Modality	Total No. of Patients	No. of Patients with at Least One False-Positive Lesion		
		Reader 1	Reader 2	Reader 3
Precontrast T1-weighted and T2-weighted MR imaging	131	44 (33.6)	38 (29.0)	49 (37.4)
Combined pre- and postcontrast MR imaging	131	49 (37.4)	40 (30.5)	44 (33.6)
Postcontrast MR imaging	131	61 (46.6)	43 (32.8)	56 (42.7)
Helical CT	127	57 (44.9)	46 (36.2)	55 (43.3)
Precontrast T1-weighted MR imaging	131	40 (30.5)	34 (26.0)	39 (29.8)
Postcontrast T1-weighted MR imaging	131	45 (34.4)	40 (30.5)	47 (35.9)

Note.—Numbers in parentheses are percentages.

familiar with image interpretation than the blinded reviewers would be. Despite this, the maximum sensitivities for MR imaging and CT were 78% and 73%, respectively. Thus, there remains considerable room for improvement of these noninvasive technologies for hepatic lesion detection.

There have not been direct comparisons between the efficacy of Gd-EOB-DTPA and the efficacy of other liver-specific MR imaging contrast agents. The results of multicenter trials of ferumoxides indicate a sensitivity range of 68%–97% (13–19); higher values correspond to single center trials. Postcontrast MR imaging with mangafodipir trisodium has been reported to have sensitivities of 72%–90% (1,2,15). Without a direct comparison trial, it is not possible to compare the results of this trial with earlier data in the literature. Vogl et al (6), however, compared gadopentetate dimeglumine with Gd-EOB-DTPA in 31 patients; in their study, Gd-EOB-DTPA allowed improved lesion detection compared with gadopentetate dimeglumine. This type of study is extremely useful in establishing the rationale for using both dynamic and delayed phase MR imaging to improve the performance of MR imaging of the liver.

There were several limitations of this study. First, helical CT was used for comparison. The helical CT scanners that are currently used are four- and 16–detector row scanners, but these were not generally available at the time of the data collection. Further improvement in the performance of CT could be possible by using newer multi–detector row scanners combined with decreased section collimation. Kawata et al (20) evaluated the potential for improved lesion detection with decreased collimation in hepatocellular carcinoma. They found that lesion detection was not significantly improved for a section collimation of <5 mm (20). Similar results were obtained for hepatic metastases (21). An additional limitation is that the full effect of the delayed hepatocyte-specific phase of imaging was not examined separately in this study. Instead, as would be the case in a clinical setting, all postcontrast MR images were interpreted together.

Overall, the study bias is clearly that of a surgically eligible population; therefore, the results may not be applicable to a more generalized patient population. A surgically eligible population was selected because of the need to obtain histopathologic confirmation of the lesions as a standard of reference. In addition, intraoperative US of the liver was used to examine liver segments that were not resected. Although the use of intraoperative US has generally been taken to be a surrogate for histologic analysis of nonresected liver segments (22–28), this technique remains an imperfect standard of reference (29,30). Intraoperative US is also operator dependent. Follow-up CT or MR imaging could be performed, but this approach requires broad assumptions regarding tumor doubling times to distinguish between new and preexisting micrometastases. Finally, of the 169 patients who received Gd-EOB-DTPA, 31 (18.3%) did not undergo a standard of reference procedure (ie, surgery, intraoperative US, and/or 3-month follow-up). This dropout rate was expected. The sample size of the enrollment population was

TABLE 6
Number of False-Positive Liver Lesions Detected by Blinded Readers and Unblinded Site Investigators

Reader	All Lesions	Lesions ≥1 cm	Lesions <1 cm	No. of Lesions Classified as Malignant*
Unblinded site investigators				
Precontrast T1-weighted and T2-weighted MR imaging	67	25	42	41 (61)
Postcontrast MR imaging	73	22	51	39 (53)
Helical CT	70	27	43	38 (54)
Reader 1				
Precontrast T1-weighted and T2-weighted MR imaging	84	42	42	64 (76)
Combined pre- and postcontrast MR imaging	79	25	54	51 (64)
Postcontrast MR imaging	103	40	63	78 (75.7)
Helical CT	106	44	62	62 (58.5)
Precontrast T1-weighted MR imaging	70	44	26	62 (88)
Postcontrast T1-weighted MR imaging	81	40	41	66 (81)
Reader 2				
Precontrast T1-weighted and T2-weighted MR imaging	66	31	35	33 (50)
Combined pre- and postcontrast MR imaging	70	24	46	37 (53)
Postcontrast MR imaging	77	25	52	42 (54)
Helical CT	84	21	63	22 (26)
Precontrast T1-weighted MR imaging	52	32	20	26 (50)
Postcontrast T1-weighted MR imaging	63	27	36	35 (56)
Reader 3				
Precontrast T1-weighted and T2-weighted MR imaging	74	29	45	31 (42)
Combined pre- and postcontrast MR imaging	71	21	50	30 (42)
Postcontrast MR imaging	94	34	60	39 (41)
Helical CT	91	33	58	34 (37)
Precontrast T1-weighted MR imaging	65	39	26	37 (57)
Postcontrast T1-weighted MR imaging	89	48	41	58 (65)

* Numbers in parentheses are percentages.

TABLE 7
Number of Liver Lesions Correctly Detected and Classified as Benign or Malignant by Blinded Readers at CT and MR Imaging

Modality	Malignant Lesions			Benign Lesions		
	<1 cm	≥1 cm	Total	<1 cm	≥1 cm	Total
			Reader 1			
Precontrast MR imaging						
T1-weighted and T2-weighted	13/56 (23)	135/176 (76.7)	148/232 (63.8)	9/39 (23)	19/40 (48)	28/79 (35)
T1-weighted	13/56 (23)	110/176 (62.5)	123/232 (53.0)	3/39 (8)	11/40 (28)	14/79 (18)
Postcontrast MR imaging						
T1-weighted and T2-weighted	23/56 (41)	146/176 (83.0)	169/232 (72.8)	16/39 (41)	22/40 (55)	38/79 (48)
T1-weighted	22/56 (39)	137/176 (77.8)	159/232 (68.5)	9/39 (23)	14/40 (35)	22/79 (28)
Pre- and postcontrast MR imaging	21/56 (38)	143/176 (81.3)	164/232 (70.7)	20/39 (51)	23/40 (58)	43/79 (54)
Helical CT	13/47 (28)	134/168 (79.8)	147/215 (68.4)	9/39 (23)	25/40 (62)	34/79 (43)
			Reader 2			
Precontrast MR imaging						
T1-weighted and T2-weighted	10/56 (18)	131/176 (74.4)	141/232 (60.8)	14/39 (36)	18/40 (45)	32/79 (40)
T1-weighted	9/56 (16)	105/176 (59.6)	114/232 (49.1)	6/39 (15)	8/40 (20)	14/79 (18)
Postcontrast MR imaging						
T1-weighted and T2-weighted	19/56 (34)	147/176 (83.5)	166/232 (71.6)	17/39 (44)	18/40 (45)	35/79 (44)
T1-weighted	16/56 (29)	125/176 (71.0)	141/232 (60.8)	7/39 (18)	8/40 (20)	15/79 (19)
Pre- and postcontrast MR imaging	18/56 (32)	135/176 (76.7)	153/232 (65.9)	14/39 (36)	29/40 (72)	43/79 (54)
Helical CT	9/47 (19)	127/168 (75.6)	136/215 (63.2)	11/39 (28)	20/40 (50)	31/79 (39)
			Reader 3			
Precontrast MR imaging						
T1-weighted and T2-weighted	11/56 (20)	119/176 (67.6)	130/232 (56.0)	14/39 (36)	20/40 (50)	34/79 (43)
T1-weighted	10/56 (18)	110/176 (62.5)	120/232 (51.7)	5/39 (13)	12/40 (30)	17/79 (22)
Postcontrast MR imaging						
T1-weighted and T2-weighted	13/56 (23)	134/176 (76.1)	137/232 (59.0)	16/39 (41)	22/40 (55)	38/79 (48)
T1-weighted	11/56 (20)	131/176 (74.4)	142/232 (61.2)	8/39 (20)	11/40 (28)	19/79 (24)
Pre- and postcontrast MR imaging	16/56 (29)	138/176 (78.4)	154/232 (66.4)	16/39 (41)	27/40 (68)	43/79 (54)
Helical CT	5/47 (11)	124/168 (73.8)	129/215 (60.0)	11/39 (28)	18/40 (45)	29/79 (37)

Note.—Numbers in parentheses are percentages.

increased to account for patient drop-out as a result of a lack of surgery owing to inoperable disease, as well as an expected lack of completion of all imaging examinations. These factors further indicate a bias toward a surgically eligible patient population.

In conclusion, MR imaging with Gd-EOB-DTPA demonstrated improved sensitivity for lesion detection compared with precontrast MR imaging for the majority of blinded readers. The contrast agent was safe in this patient population.

Acknowledgments: The complete list of authors is David A. Bluemke, MD, PhD; Dushyant Sahani, MD; Marco Amendola, MD; Thomas Balzer, MD; Josy Breuer, MD; Jeffrey J. Brown, MD; David D. Casalino; Peter L. Davis, MD; Isaac R. Francis, MD; Glenn Krinsky, MD; Fred T. Lee, Jr, MD; David Lu, MD; Erik K. Paulson, MD; Lawrence H. Schwartz, MD; Evan S. Siegelman, MD; William C. Small, MD; Therese M. Weber, MD; Adam Welber, MS, MD; and Kohkan Shamsi, MD. The authors acknowledge Eileen P. Hanna for supervision of study conduct and R. Carter for organization and management of the off-site evaluation.

Author affiliations: Johns Hopkins University School of Medicine, Baltimore, Md (D.A.B.); Massachusetts General Hospital, Boston, Mass (D.S.); University of Miami School of Medicine, Miami, Fla (M.A.); Berlex Laboratories, Montville, NJ (T.B., K.S.); Schering AG, Berlin, Germany (J.B.); Mallinckrodt Institute of Radiology, St Louis, Mo (J.J.B.); University of Chicago Hospital, Chicago, Ill (D.D.C.); Presbyterian University Hospital, Pittsburgh, Pa (P.L.D.); University of Michigan Health System, Ann Arbor, Mich (I.R.F.); New York University Medical Center, New York, NY (G.K., A.W.); University of Wisconsin Hospitals & Clinics, Madison, Wis (F.T.L.); University of California, Los Angeles, Calif (D.L.); Duke University Medical Center, Durham, NC (E.K.P.); Memorial Sloan-Kettering Cancer Center, New York, NY (L.H.S.); Hospital of the University of Pennsylvania, Philadelphia (E.S.S.); Emory University Hospital, Atlanta, Ga (W.C.S.); and University of Alabama, Birmingham, Ala (T.M.W.).

References

1. Braga HJ, Choti MA, Lee VS, Paulson EK, Siegelman ES, Bluemke DA. Liver lesions: manganese-enhanced MR and dual-phase helical CT for preoperative detection and characterization comparison with receiver operating characteristic analysis. Radiology 2002;223:525–531.
2. Federle M, Chezmar J, Rubin DL, et al. Efficacy and safety of mangafodipir trisodium (MnDPDP) injection for hepatic MRI in adults: results of the U.S. multicenter phase III clinical trials—efficacy of early imaging. J Magn Reson Imaging 2000;12: 689–701.
3. Reimer P, Rummeny EJ, Shamsi K, et al. Phase II clinical evaluation of Gd-EOB-DTPA: dose, safety aspects, and pulse sequence. Radiology 1996;199:177–183.
4. Hamm B, Staks T, Muhler A, et al. Phase I clinical evaluation of Gd-EOB-DTPA as a hepatobiliary MR contrast agent: safety, pharmacokinetics, and MR imaging. Radiology 1995;195:785–792.
5. Reimer P, Rummeny EJ, Daldrup HE, et al. Enhancement characteristics of liver metastases, hepatocellular carcinomas, and hemangiomas with Gd-EOB-DTPA: preliminary results with dynamic MR imaging. Eur Radiol 1997;7:275–280.
6. Vogl TJ, Kummel S, Hammerstingl R, et al. Liver tumors: comparison of MR imaging with Gd-EOB-DTPA and Gd-DTPA. Radiology 1996;200:59–67.
7. Couinaud C. Surgical anatomy of the liver: several new aspects [in French]. Chirurgie 1986;112:337–342.
8. Carlos RC, Hussain HK, Song JH, Francis IR. Gadolinium-ethoxybenzyl-diethylenetriamine pentaacetic acid as an intrabiliary contrast agent: preliminary assessment. AJR Am J Roentgenol 2002;179:87–92.
9. Bollow M, Taupitz M, Hamm B, Staks T, Wolf KJ, Weinmann HJ. Gadolinium-ethoxybenzyl-DTPA as a hepatobiliary contrast agent for use in MR cholangiography: results of an in vivo phase-I clinical evaluation. Eur Radiol 1997;7:126–132.
10. Goldstein HA, Kashanian FK, Blumetti RF, Holyoak WL, Hugo FP, Blumenfield DM. Safety assessment of gadopentetate dimeglumine in U.S. clinical trials. Radiology 1990;174:17–23.
11. Aslanian V, Lemaignen H, Bunouf P, Svaland MG, Borseth A, Lundby B. Evaluation of the clinical safety of gadodiamide injection, a new nonionic MRI contrast medium for the central nervous system: a European perspective. Neuroradiology 1996; 38:537–541.
12. Rubin DL, Desser TS, Semelka R, et al. A multicenter, randomized, double-blind study to evaluate the safety, tolerability, and efficacy of OptiMARK (gadoversetamide injection) compared with Magnevist (gadopentetate dimeglumine) in patients with liver pathology: results of a phase III clinical trial. J Magn Reson Imaging 1999;9:240–250.
13. del Frate C, Bazzocchi M, Mortele KJ, et al. Detection of liver metastases: comparison of gadobenate dimeglumine-enhanced and ferumoxides-enhanced MR imaging examinations. Radiology 2002; 225:766–772.
14. Choi D, Kim S, Lim J, et al. Preoperative detection of hepatocellular carcinoma: ferumoxides-enhanced MR imaging versus combined helical CT during arterial portography and CT hepatic arteriography. AJR Am J Roentgenol 2001;176:475–482.
15. Kim SK, Kim SH, Lee WJ, et al. Preoperative detection of hepatocellular carcinoma: ferumoxides-enhanced versus mangafodipir trisodium-enhanced MR imaging. AJR Am J Roentgenol 2002;179:741–750.
16. Raman SS, Lu DS, Chen SC, Sayre J, Eilber F, Economou J. Hepatic MR imaging using ferumoxides: prospective evaluation with surgical and intraoperative sonographic confirmation in 25 cases. AJR Am J Roentgenol 2001;177:807–812.
17. Bluemke DA, Paulson EK, Choti MA, DeSena S, Clavien PA. Detection of hepatic lesions in candidates for surgery: comparison of ferumoxides-enhanced MR imaging and dual-phase helical CT. AJR Am J Roentgenol 2000;175:1653–1658.
18. Ros PR, Freeny PC, Harms SE, et al. Hepatic MR imaging with ferumoxides: a multicenter clinical trial of the safety and efficacy in the detection of focal hepatic lesions. Radiology 1995;196:481–488.
19. Bluemke DA, Weber TM, Rubin D, et al. Hepatic MR imaging with ferumoxides: multicenter study of safety and effectiveness of direct injection protocol. Radiology 2003;228:457–464.
20. Kawata S, Murakami T, Kim T, et al. Multidetector CT: diagnostic impact of slice thickness on detection of hypervascular hepatocellular carcinoma. AJR Am J Roentgenol 2002;179:61–66.
21. Haider MA, Amitai MM, Rappaport DC, et al. Multi-detector row helical CT in preoperative assessment of small (≤1.5 cm) liver metastases: is thinner collimation better? Radiology 2002;225:137–142.
22. Knol JA, Marn CS, Francis IR, Rubin JM, Bromberg J, Chang AE. Comparisons of dynamic infusion and delayed computed tomography, intraoperative ultrasound, and palpation in the diagnosis of liver metastases. Am J Surg 1993;165:81–87.
23. Zacherl J, Pokieser P, Wrba F, et al. Accuracy of multiphasic helical computed tomography and intraoperative sonography in patients undergoing orthotopic liver transplantation for hepatoma: what is the truth? Ann Surg 2002;235:528–532.
24. Cervone A, Sardi A, Conaway GL. Intraoperative ultrasound (IOUS) is essential in the management of metastatic colorectal liver lesions. Am Surg 2000;66:611–615.
25. Milsom JW, Jerby BL, Kessler H, Hale JC, Herts BR, O'Malley CM. Prospective, blinded comparison of laparoscopic ultrasonography vs. contrast-enhanced computerized tomography for liver assessment in patients undergoing colorectal carcinoma surgery. Dis Colon Rectum 2000;43:44–49.
26. Schmidt J, Strotzer M, Fraunhofer S, Boedeker H, Zirngibl H. Intraoperative ultrasonography versus helical computed tomography and computed tomography with arterioportography in diagnosing colorectal liver metastases: lesion-by-lesion analysis. World J Surg 2000;24:43–47.
27. Goletti O, Celona G, Galatioto C, et al. Is laparoscopic sonography a reliable and sensitive procedure for staging colorectal cancer? a comparative study. Surg Endosc 1998;12:1236–1241.
28. Fortunato L, Clair M, Hoffman J, et al. Is CT portography (CTAP) really useful in patients with liver tumors who undergo intraoperative ultrasonography (IOUS)? Am Surg 1995;61:560–565.
29. Foley EF, Kolecki RV, Schirmer BD. The accuracy of laparoscopic ultrasound in the detection of colorectal cancer liver metastases. Am J Surg 1998;176:262–264.
30. Takeuchi N, Ramirez JM, Mortensen NJ, Cobb R, Whittlestone T. Intraoperative ultrasonography in the diagnosis of hepatic metastases during surgery for colorectal cancer. Int J Colorectal Dis 1996;11:92–95.